TEXAS TECH UNIVERSITY
Natural Science Research Laboratory

Occasional Papers

Museum of Texas Tech University Number 367 4 August 2020

Evidence from Mitochondrial DNA Sequences Suggest a Recent Origin for *Peromyscus truei comanche*

Emily A. Wright, Emma K. Roberts, Courtney L. Evans, David J. Schmidly, and Robert D. Bradley

Abstract

Isolated populations of *Peromyscus truei comanche* occur in the Tule and Palo Duro Canyon region of the Texas Panhandle. Four plausible routes that may explain the current distribution of the piñon mouse were investigated herein by comparing the phylogenetic relationships of *P. t. comanche* with eight other subspecies of *P. truei* from throughout the western and southwestern United States and the Baja Peninsula of Mexico. To determine the origin and affiliation of *P. t. comanche* populations, DNA sequence data were obtained from the mitochondrial cytochrome-*b* gene (1,143 bp) and displacement loop (971 bp) and analyzed in a phylogenetic context. Results of the Bayesian inference analyses indicated that samples of *P. t. comanche* genetically were undifferentiated from two of the eight subspecies of *P. truei* (*P. t. nevadensis* and *P. t. truei*). Overall, genetic divergence values, obtained from the cytochrome-*b* gene, ranged from 1.16% to 4.99% between *P. t. comanche* and the other eight subspecies of *P. truei*. *Peromyscus truei comanche* differed genetically from the nearest population of *P. t. truei* (Glenrio, Texas) by 1.73%; however, samples of *P. t. comanche* were differentiated from individual populations of *P. t. truei* from Mills Canyon, New Mexico, Black Mesa, Oklahoma, and Guadalupe Mountains National Park, Texas by 0.79%, 1.00%, and 2.00%, respectively. Although results of the phylogenetic analyses were unable to definitively explain the origin of *P. t. comanche*, levels of genetic divergence suggest a recent evolutionary history with samples from Mills Canyon, New Mexico. Results from the divergence dating analyses suggest that *P. t. comanche* from the Texas Panhandle diverged from a source-stock population in northeastern New Mexico approximately 0.71 mya. This infers an expansion route (Route II) from Mills Canyon, New Mexico, along canyonlands associated with the Canadian River system to the northeastern edge of the Llano Estacado, and subsequent isolation and divergence of *P. t. comanche* from its *P. t. truei*-like ancestor; whereas the closest extant populations of *P. t. truei* in Glenrio, Texas genetically were more divergent (1.73%), and also would have required dispersal across the inhospitable landscape (for *P. truei*) of the Llano Estacado. Finally, *P. t. comanche* did not form a monophyletic group (to the exclusion of other samples of *P. t. truei*) in the genetic analyses, however the significant levels of morphological differentiation reported in other studies justifies its retention as a valid subspecies.

Key words: cytochrome-*b* gene, dispersal, displacement loop, Llano Estacado, *Peromyscus truei comanche*, phylogenetics, stepping-stone hypothesis, vicariance

INTRODUCTION

Peromyscus truei occurs throughout the southwestern United States and portions of Sonora and Baja California del Norte, Mexico (Hoffmeister 1981; Durish et al. 2004). Described by Blair (1943), *P. t. comanche* geographically is isolated along the rocky, juniper slopes of northern and eastern peripheral edges of the Llano Estacado, specifically in Randall, Armstrong, and Briscoe counties of the Tule and Palo Duro Canyon areas of the Texas Panhandle (Blair 1943; Choate 1991, 1997). *P. t. comanche* prefers more precipitous rocky areas along the escarpment and thus a microhabitat separation exists between *P. t. comanche* and other sympatric species such as *P. attwateri* and *P. leucopus* (Choate 1991, 1997; Choate et al. 1991). This region, referred to as the 'Break of the Plains', contains cedar forests on the canyon slopes and serves as a suitable habitat for a specialist rodent like the piñon mouse (Schmidly 1973).

The occurrence and explanation for the distribution of *P. t. comanche* has proven to be enigmatic. Although several populations of *P. t. comanche* occur along the northeastern side of the Llano Estacado, (Choate 1991, 1997; Durish et al. 2004; Schmidly and Bradley 2016), the nearest additional populations of *P. truei*, excluding the Tule and Palo Duro Canyon localities, are samples located in Deaf Smith County (south of Glenrio, Texas; Choate 1997; Choate et al. 1991) and Quay County (SE of Tucumcari, New Mexico; Findley et al. 1975; Hall 1981) at the interface of the western edge of the Llano Estacado and Canadian River Canyon and extreme western Oklahoma (Tesquite Canyon and Kenton region; Caire et al. 1989; Hall 1981).

The aforementioned samples from eastern New Mexico, western Oklahoma, and northwestern Texas have been assigned to *P. t. truei* (Hall 1981; Choate 1997; Choate et al. 1991; Schmidly and Bradley 2016). These localities are 120–180 km W and 300 km NNW, respectively from the type locality of *P. t. comanche* near Tule and Palo Duro Canyons, Briscoe County, Texas. How *P. t. comanche* populated the northern and eastern edge of the Llano Estacado is unknown; however, given its proximity to populations of *P. t. truei* near the New Mexico/Texas border (circa Glenrio and Tucumcari) and western Oklahoma (circa Black Mesa), it is possible either the western or northwestern populations of *P. t. truei* may have served as the ancestral population of *P. t. comanche*.

Blair (1943) described *P. t. comanche* as a distinct species (*P. comanche*) based on a series of 92 specimens collected from the Tule and Palo Duro Canyon region of the Texas Panhandle. Blair's description was based on the observation that *P. comanche* possessed: smaller auditory bullae; a shorter ear relative to hindfoot; and a significantly longer tail than did other members of the piñon deermouse, *P. truei* (Blair 1943). In Hoffmeister's (1951) review of the *P. truei* species group, *P. comanche* was relegated to a subspecies of *P. nasutus* based on coloration, a uniquely shaped interparietal, and larger auditory bullae. Hoffmeister and de la Torre (1961) split *P. difficilis* and *P. nasutus* into different species with *P. n. comanche* relegated to subspecific status within *P. difficilis* due to its relatively small ears, shorter tail, and small auditory bullae. Johnson and Packard (1974), based on results of an allozyme study, determined that *P. comanche* genetically was most closely affiliated with *P. truei*. Further, although they found no apparent fixed allozymic differences between *P. comanche* and *P. truei*, they concluded that *P. comanche* should be considered as a species distinct from *P. truei*. Conversely, based on morphologic and karyotypic data, Schmidly (1973) and Modi and Lee (1984) retained *P. t. comanche* as a subspecies of *P. truei*.

Using haplotype patterns developed from restriction digests of the mitochondrial genome, DeWalt et al. (1993) argued that *P. t. comanche* should remain a subspecies of *P. truei*. Similarly, Durish et al. (2004) sequenced the mitochondrial cytochrome-*b* (*Cyt*b) gene and reported that individuals of *P. t. comanche* differed from individuals of *P. t. truei* collected from New Mexico, Arizona, and California by a genetic divergence of 1.20%. Although Durish et al. (2004) agreed with Modi and Lee (1984), Dewalt et al. (1993), and

Schmidly (1973) that *P. t. comanche* should continue to be recognized as a member of *P. truei*, unfortunately, they were unable to examine specimens of *P. t. truei* from nearby populations in western Texas, eastern New Mexico, or extreme western Oklahoma to help establish a phylogenetic connection of *P. t. comanche* to the more western and northern populations. Furthermore, they did not offer any comments on whether *P. t. comanche* was a valid subspecies of *P. truei* or whether it should be subsumed into *P. t. truei*, the geographically closest population.

Recent evidence presented by Rogers et al. (2019) suggested that the systematics of *P. truei* are more complex than reported in these previous studies. Their work, using DNA sequence and morphologic data, indicated that *P. truei*, as currently recognized, may be comprised of multiple species, including western and eastern phylogroups. Furthermore, based on their data, *P. t. comanche* was aligned with the more eastern phylogroup, which includes portions of *P. t. truei* and *P. t. nevadensis* (Rogers et al. 2019).

In addition to the uncertain phylogenetic placement of *P. t. comanche*, the origin of the Tule and Palo Duro Canyon population is not clear, although there seem to be two possibilities, one of which is that *P. t. comanche* populations successfully dispersed via a "stepping-stone model", presumably from nearby populations in eastern New Mexico/western Texas or from western Oklahoma. Under this model, adequate habitat patches would facilitate movement from one population to another; thereby, successfully providing temporary refugia for subsequent dispersal and expansion to more optimal habitat (Yang et al. 2016). Kimura (1953) and Kimura and Weiss (1964) suggested that the stepping-stone model would explain movement of individuals along fragmented habitat and this scenario would support documented distributions for *P. t. comanche* along the escarpments and edges of the Llano Estacado and into the Tule and Palo Duro Canyon area.

Two possible scenarios can be proposed to explain the present-day distribution of *P. t. comanche*. Under the first scenario, individuals presumably may have dispersed (via stepping-stone model) from western Texas, northeastern New Mexico or western Oklahoma. These putative routes of dispersal (IA, IB, II, III, and IV), or some combination thereof, are shown in Figure 1. Route I (Glenrio, Texas to the Tule and Palo Duro Canyon region) represents the most plausible dispersal route, although it would require individuals of *P. t. truei* to traverse 120 km across unsuitable habitat. Routes IIA and IIB (northeastern New Mexico to the Tule and Palo Duro Canyon region) depict potential pathways, with *P. t. truei* presumably dispersing either: IIA) northeast following the edges of the Canadian River system and, subsequently, south following the eastern edges of the Llano Estacado into Palo Duro Canyon; or IIB) following the Canadian River system to other tributary systems (major: Palo Duro and Tierra Blanca creeks; minor: Timber, Sunday, and Canyon Cita creeks; see Gould 1907) in a southeasterly direction, directly leading into Palo Duro Canyon. Route III (Black Mesa to the Tule and Palo Duro Canyon region) depicts an alternative pathway of dispersal along the edges of the Wichita and Amarillo Mountain Uplifts to the northeastern edges of the Llano Estacado southward into Tule and Palo Duro Canyon. Route IV (Guadalupe Mountains National Park to the Tule and Palo Duro Canyon region) describes a final pathway along the southwestern and southeastern edges of the Llano Estacado northward to the southern distribution of *P. t. comanche* populations.

A second scenario (vicarience) would suggest that *P. t. comanche* was a relictual population that originally was a widespread population and subsequently became isolated during the development of the Llano Estacado. Uplifts of the Rocky Mountains during the Cenozoic (70 million years ago [mya]), produced the materials underlying the Llano Estacado, and subsequent erosion and weathering to the Rocky Mountains by the Pecos and Canadian rivers generated the canyonland landscape in which *P. t. comanche* resides (Choate 1991, 1997). Initial separation due to these aforementioned geographical barriers to dispersal along with *P. truei* specialist tendencies (e.g. preference for rocky outcroppings and canyon slopes), in recent times, may have further isolated populations of *P. truei* along the northeastern edge of the Llano Estacado followed by a divergence into *P. t. comanche*.

To discern among these two scenarios, a combination of mitochondrial markers (*Cyt*b; displacement loop, D-loop) and phylogenetic analyses were used to determine the origin of *P. t. comanche* relative to other geographically proximal populations. The objectives

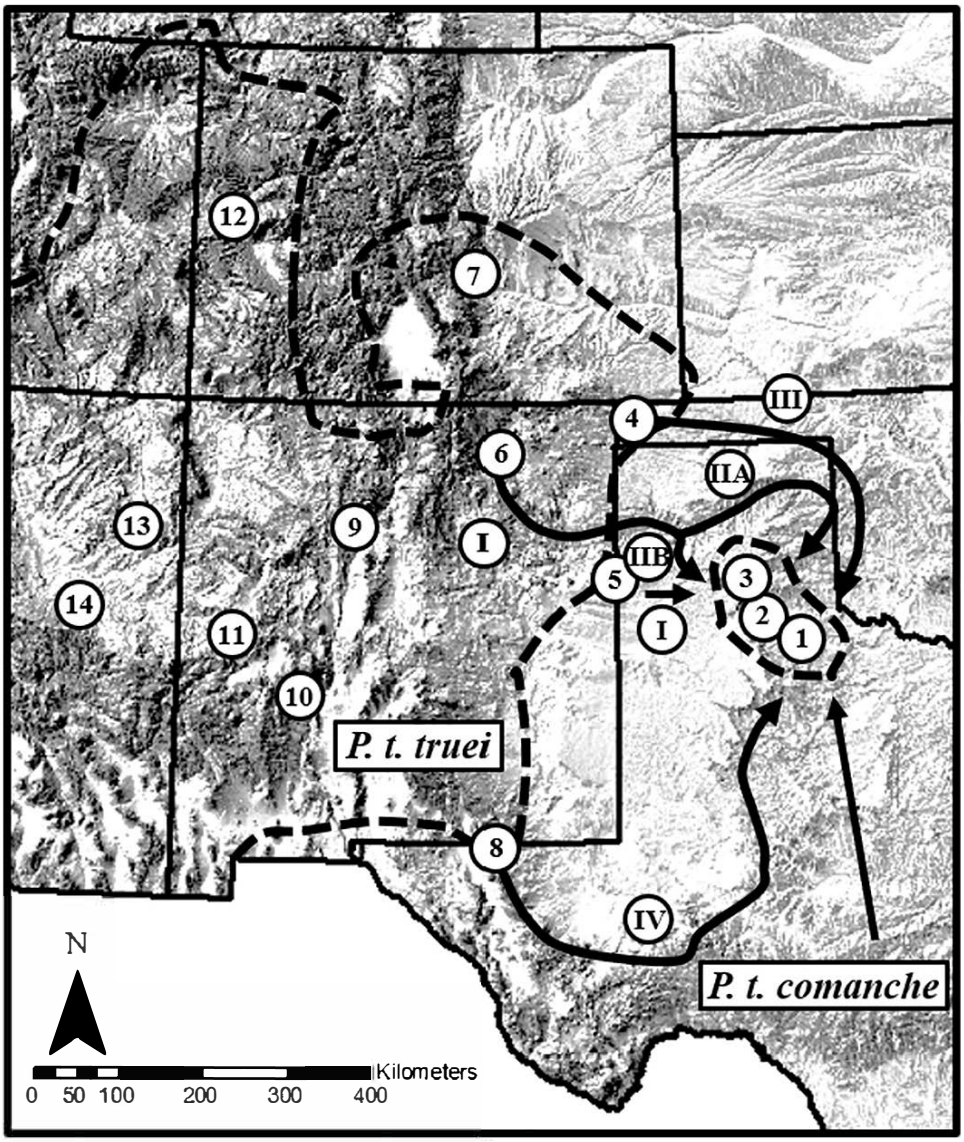

Figure 1. Sampling localities for selected individuals of *P. truei* examined in this study. Samples from GenBank, including Rogers et al. (2019), are not depicted. Numbers contained in white circles indicate localities from Texas and surrounding states. Roman numerals (I, IIA, IIB, III, and IV) indicate hypothetical pathways for *P. truei* dispersal onto the Llano Estacado and surrounding canyonlands. Dashed lines indicate the distribution of *P. t. truei* and *P. t. comanche*. Refer to the Appendix for a complete list of specimens examined.

of this study were to: 1) investigate the potential geographic impact of the Llano Estacado on the current distribution of *P. truei*; and 2) determine if the Tule and Palo Duro Canyon populations are more closely aligned with populations to the west, northwest, or southwest, or are they a relict of a once more broadly distributed *P. truei*. In addition, molecular data were used to determine which of the scenarios, stepping-stone or vicariance, explains the disjunct distribution of *P. t. comanche*.

MATERIALS AND METHODS

Sampling.—Individuals (n = 162) representing nine subspecies of *P. truei* were collected from naturally-occurring populations in the western United States and Mexico, 28 of which were borrowed from the Natural Science Research Laboratory, Museum of Texas Tech University and 134 were incorporated from other molecular studies (e.g., GenBank). Specimens were collected following methods outlined in the guidelines of the American Society of Mammalogists (Sikes et al. 2016) and approved by the Texas Tech University Animal Care and Use Committee. To determine the source-stock of *P. t. comanche*, samples of *P. t. truei* from Mills Canyon, New Mexico; Black Mesa State Park and Nature Preserve, Oklahoma; Glenrio, Texas; and Guadalupe Mountains National Park, Texas, were used to represent the closest known populations to the current distribution of *P. t. comanche*. For the *Cyt*b dataset (see Appendix), reference sequences (*P. attwateri*, *gratus*, *nasutus*, and *truei*) were obtained from the following studies: 117 individuals (Rogers et al. 2019), 9 individuals (Durish et al. 2004), 3 individuals (Rodhouse et al. 2010), 3 individuals including *P. attwateri* as outgroup taxon (Tiemann-Boege et al. 2000), 1 individual (Bradley et al. 2004), and 1 individual (Smith and Patton 1999). For the D-loop dataset, 35 individuals (see Appendix) were sequenced following the methods of Castro-Campillo et al. (1999). All sequences (*Cyt*b and D-loop) generated herein were deposited in GenBank and are listed in the Appendix.

DNA sequencing.—For *Cyt*b sequences, genomic DNA was isolated from 0.1g of frozen liver tissue using the Qiagen DNeasy kit (Qiagen Inc., Valencia, California). For all samples the full length *Cyt*b gene (1,143 bp) was amplified using polymerase chain reaction (PCR) methodology following Saiki et al. (1988) with the amplification primers: LGL765 (forward, Bickham et al. 1995) and LGL766 (reverse, Bickham et al. 2004). HotStarTaq (Qiagen Inc., Valencia, California) was used in the PCR along with the following thermal profile: hot start of 80°C, initial denaturation at 95°C for 2 min, followed by 34 cycles of denaturation at 95°C for 30 s, annealing (range: 44–45°C) for 45 s, extension at 73°C for 1 min, and a final extension at 73°C for 15 min.

Tissue samples were unavailable for the specimens from Glenrio and Guadalupe Mountains National Park, Texas; therefore, a small piece of a toe (approximately 5 mg excluding the toenail) was obtained from four (two from each locality) museum voucher specimens. DNA was isolated following a modification of methods reported in Curry and Derr (2019). Toes initially were cleaned using a 95% ethanol rinse and then immediately treated with UV irradiation for 5 min. Each toe clip was washed with ddH_2O and incubated at 56°C for 15 minutes (3 repetitions). Genomic DNA was isolated using the Quick-DNA Universal Kit (Zymo Research, Irvine, California). A 423 bp fragment (position 400–823 bp aligned) of the *Cyt*b gene was amplified using PCR methods with primers 400F (Edwards et al. 2001) and 700H (Peppers and Bradley 2000), HotStarTaq (Qiagen Inc., Valencia, California) and the same thermal profile as described above for the tissue samples with the exception that the annealing temperature was 50°C.

All PCR products were purified with either ExoSAP-IT or a Qiagen PCR Purification Kit (Applied Biosystems, Foster City, California and Qiagen Inc., Valencia, California). Cycle sequence primers included LGL765, LGL766, 870R, and F1 (Peppers et al. 2002; Whiting et al. 2003) and subsequent cycle sequencing reactions were purified using the ABI Prism Big Dye version 3 terminator ready reaction mix (Applied Biosystems, Foster City, California). Sequencing reactions were purified using Sephadex columns (Princeton Separation, Adelphia, New Jersey) and centrifugation, followed by dehydration and resuspension in formamide. Purified products were analyzed on an ABI Prism 310 automated sequencer (Biotechnology Resource Center, Institute of Biotechnology, Cornell University, Ithaca, New York). Resulting sequences were aligned and proofed with Sequencher 4.10.1 software (Gene Codes Corporation, Ann Arbor, Michigan) and chromatograms were inspected to authenticate any base changes.

The mtDNA D-loop was amplified using a similar methodology as described above. The differences in sequencing methods for D-loop are described below. Primers utilized to amplify the full-length D-loop (971 bp) were 2340-4 (forward, Bickham et al. 1995) and 2340-5 (reverse, Castro-Campillo et al. 1999). Thermal profiles for PCR were as follows: a hot start of 80°C, initial denaturation at 95°C for 2 min, followed

by 35 cycles of denaturation at 95°C for 30 s, annealing (range: 48–49°C) for 45 s, and extension at 72°C for 1 min, with a final extension at 72°C for 15 min. Primers used to cycle sequence the products included 2340-4, 2340-5, 500F, and 1115 (Méndez-Harclerode et al. 2005).

Phylogenetic analyses.—For the *Cyt*b gene, a parsimony analysis was conducted using PAUP* 4.0a166 (Swofford 2003) on an initial dataset containing 523 individuals. Nucleotide positions were treated as unordered, discrete characters with four possible states: A, C, G, and T. Verification of taxonomic assignment, elimination of duplicate haplotypes, and confirmation of monophyletic clades resulted in a final dataset of 162 individuals for subsequent analyses. *Peromyscus attwateri*, the sister taxon to *P. truei* (Durish et al. 2004), was incorporated as the outgroup taxon.

jModelTest-2.1.10 (Darriba et al. 2012) identified GTR+G and TIM3+I+G as the most appropriate model of evolution for *Cyt*b and D-loop, respectively. To perform likelihood analysis under a Bayesian inference model, MrBayes v.3.2.6 (Ronquist et al. 2012) was run with the following parameters: 2 independent runs with four chains, one cold and three heated (MCMCMC), 10 million generations, and sample frequency every 1,000th generation from the last nine million generated. A consensus tree (50% majority rule) was constructed from the remaining trees, and posterior probability values (PPV) were estimated to provide nodal support. PPV $\geq$ 0.95 were considered indicative of nodal support. Genetic distance values were calculated using the Kimura 2-parameter model of evolution (Kimura 1980) to assess levels of divergence between populations of *P. truei* (Arizona, Baja California, California, Colorado, Idaho, New Mexico, Oklahoma, Oregon, Texas, and Utah) and *P. t. comanche* (Texas) following Baker and Bradley (2006).

Genetic divergence and divergence dating.—Two methods were used to examine genetic divergence and molecular dating. In the first method, the Kimura 2-parameter model of evolution (Kimura 1980) was utilized to estimate genetic distances among selected taxa and haplotypes. The resulting values were used to examine levels of genetic divergence pertaining to the genetic species concept outlined in Bradley and Baker (2001) and Baker and Bradley (2006). A second method (molecular clock test; MEGA v.10, Kumar et al. 2018) was employed to define the appropriate molecular timeline and to determine whether to accept or reject a stringent molecular clock. Divergence dates for subspecies of *P. truei* were estimated from the *Cyt*b dataset (obtained in this study and GenBank, see Appendix) using the program BEAST v2.6.1 (Bouckaert et al. 2014). Divergence date estimates were not determined for the D-loop dataset due to lack of in-depth geographic and taxonomic sampling.

Fossil calibrations were placed on the *P. truei* node, based on the fossil date (~2.7 mya) from the most recent common ancestor to *P. attwateri* (Dalquest 1962; Karow et al. 1999) following methods outlined in previous studies (Schenk et al. 2013; Bouckaert et al. 2014; Ordóñez-Garza et al. 2014; Platt et al. 2015; Sullivan et al. 2017; Bradley et al. 2019). A Yule tree prior was used for the BEAST analysis and a prior lognormal distribution was placed on root height to constrain the divergence date estimates of the overall tree to ~2.7 mya with a σ value of 0.5 and to reflect the uncertainty in the fossil record. Outgroup taxa used were the same as the Bayesian analyses. Optimization of the analysis and final parameters were evaluated using initial test runs with the following parameters: GTR+I+G (nucleotide substitution model), 1.0 x 10^7 generations, and 10% burn-in. Two final runs of 2.0 X 10^7 generations were analyzed with log and tree files, which were then combined to generate divergence date estimates and produce a maximum clade credibility tree. Tracer and TreeAnnotator (Bouckaert et al. 2014) was used to examine for sufficient mixing, convergence stability, and effective sample size >200 for all parameters and to estimate the optimal phylogenetic tree, respectively.

RESULTS

Phylogenetic analyses.—Complete nucleotide sequences from the mitochondrial *Cyt*b gene (1,143 bp) and D-loop (971 bp) were obtained from 162 and 35 individuals, respectively. An initial Bayesian analysis used *P. attwateri* as the outgroup taxon in addition to *P. difficilis*, *P. nasutus*, and *P. gratus*. A secondary

Bayesian analysis only used *P. gratus* (sister taxon) as the outgroup. Both analyses produced similar topologies but only the first is reported herein. The topology of the phylogenetic tree obtained from the Bayesian analysis of the *Cyt*b dataset indicated nodal support (PPV ≥ 0.95) primarily for basal nodes; consequently, unsupported clades were collapsed so that only major supported clades were depicted (Fig. 2). Members of each species (*P. difficilis*, *P. nasutus*, *P. gratus*, and *P. truei*) were arranged as independent, monophyletic clades. Within *P. truei*, two supported clades were identified that corresponded to the western haplotype (Arizona, Baja California, California, Idaho, Nevada, Oregon, and Utah) and eastern haplotype (Arizona, Colorado, Oklahoma, New Mexico, Texas, and Utah) similar to that depicted in Rogers et al. (2019). However, relationships between members of *P. truei* subspecies and *P. t. comanche* revealed little to no genetic differentiation and no evident population structure. The Bayesian phylogenetic tree, generated using D-loop DNA sequences (Fig. 3), produced a topology in which 18 of the 30 nodes were supported with Bayesian PPV ≥ 0.95. Similar to the *Cyt*b phylogeny, members of each species group were arranged into four supported clades and within *P. truei* there was little to no genetic differentiation and structure.

Genetic distances.—For selected taxa, average genetic distance values (Table 1) were obtained from the Kimura 2-parameter model of evolution (Kimura 1980). Interspecific comparisons ranged from 7.21% to 13.30% (*Cyt*b) and 5.58% to 11.10% (D-loop) whereas intraspecific comparisons for both *Cyt*b and D-loop ranged from 1.00% to 3.00%. Average genetic distances of *Cyt*b between *P. t. comanche* and the other eight subspecies of *P. truei* ranged from 1.16% (*P. t. truei* east) to 4.99% (*P. t. chlorus*). Subspecific comparisons for the four focal populations of *P. t. truei* (Mills Canyon, Black Mesa, Glenrio, and Guadalupe Mountains National Park) to populations of *P. t. comanche* (Tule and Palo Duro Canyon region) ranged from 0.79% to 2.00% (*Cyt*b); subspecific comparisons for D-loop were only available between *P. t. comanche* and *P. t. truei* (Mills Canyon = 1.71%) and *P. t. comanche* and *P. t. truei* (Black Mesa = 1.81%).

Divergence dating.—Molecular clock tests (Kumar et al. 2018) rejected a strict molecular clock for the *Cyt*b dataset; therefore, a relaxed log normal molecular clock was used in subsequent analyses. Mean rates of evolution ($p < 0.05$) between clades depicted in the Bayesian analysis yielded a mean rate of 0.3 substitutions per site per million years (95% highest posterior density [HPD]: 0.66 to 5.20) for *Cyt*b (Fig. 4). The Yule birth rate was estimated to be 4.25 (95% HPD: 0.98 to 8.83). The divergence dating analysis indicated that the initial radiation of the western and eastern clades of *P. truei* was approximately 1.29 mya. The divergence date estimates obtained from the *Cyt*b dataset indicated that a *P. truei*-like ancestor diverged from a *P. gratus*-like ancestor approximately 1.85 mya. Within *P. truei*, the western and eastern clades appear to have diverged 1.29 mya, with the western haplotype corresponding to eight subspecies (*P. t. chlorus*, *P. t. gilberti*, *P. t. lagunae*, *P. t. martirensis*, *P. t. montipinoris*, *P. t. nevadensis*, *P. t. preblei*, and *P. t. truei*) and the eastern haplotype corresponding to three subspecies (*P. t. comanche*, *P. t. nevadensis*, and *P. t. truei*). Relative to this study, the divergence of the three closely related subspecies (*P. t. comanche*, *P. t. nevadensis*, and *P. t. truei*) contained in the eastern clade occurred approximately 0.81 mya.

DISCUSSION

Results of the *Cyt*b analyses indicated two supported clades representing a geographical designation (eastern and western) conforming to that discussed by Rogers et al. (2019). All individuals of *P. t. comanche* were included in the eastern clade along with some representatives of *P. t. nevadensis* and *P. t. truei*. However, other samples of *P. t. nevadensis* and *P. t. truei* were included as members of the western clade along with *P. t. chlorus*, *P. t. gilberti*, *P. t. lagunae*, *P. t. martirensis*, *P. t. montipinoris*, and *P. t. preblei*. Based on the results of Rogers et al. (2019) and data presented herein, individuals composing the eastern clade probably should be recognized as a single taxonomic unit distinct from those in the western clade. DNA sequences from D-loop did not contribute substantial information to the phylogenetic relationships among the nine subspecies of *P. truei* due to either the low levels of genetic divergence or lack of taxonomic sampling; consequently,

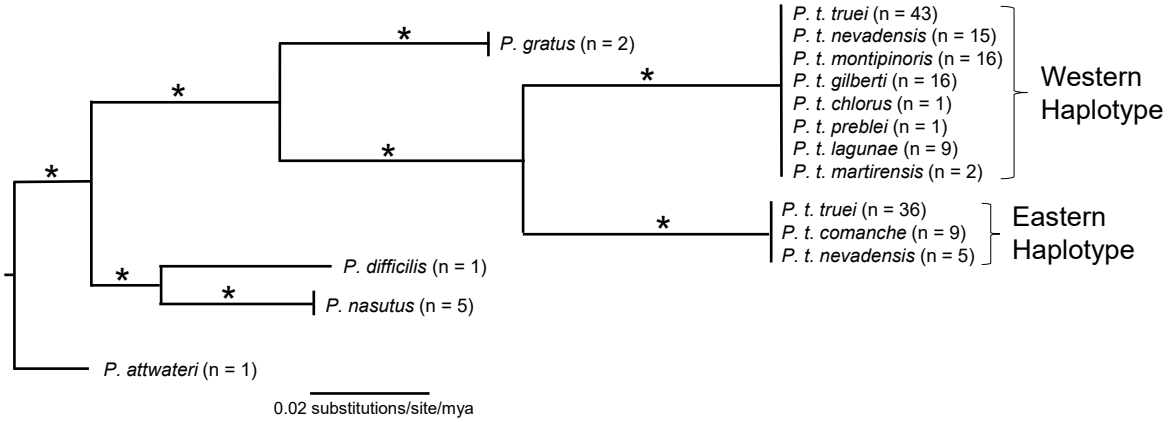

Figure 2. Phylogenetic tree generated from cytochrome-*b* sequences and Bayesian inference analyses (MrBayes 3.2; Ronquist 2012) and the GTR+G model of evolution. Posterior probability values ≥ 0.95 are indicated by an asterisk and depict nodal support. Designation of western and eastern haplotype are consistent with clades reported in Rogers et al. (2019).

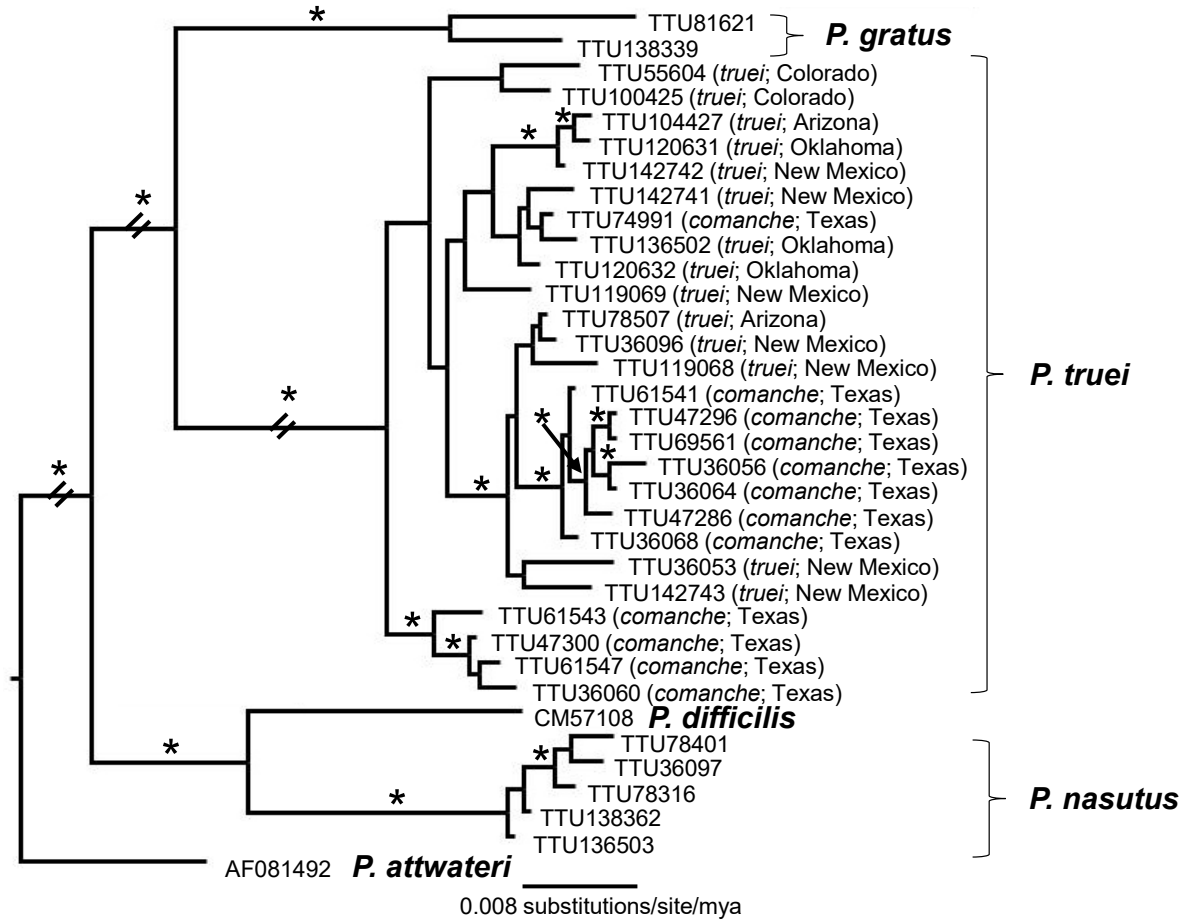

Figure 3. Phylogenetic tree generated using displacement-loop sequences and Bayesian inference analyses (MrBayes 3.2; Ronquist 2012) and the TIM3+I+G model of evolution. Posterior probability values ≥ 0.95 are indicated by an asterisk and depict nodal support.

Table 1. Average genetic distances estimated using the Kimura 2-parameter model of evolution (Kimura 1980) reported for select taxonomic groups in this study. East and west designations refer to the haplotypes defined by Rogers et al. (2019). Populations assigned to various subspecies and localities are depicted in the Appendix. Guadalupe Mountains National Park was abbreviated to GUMO.

Peromyscus comparsion	*Cyt*b	D-loop
Between species		
P. attwateri versus *P. difficilis*	8.50	7.37
P. attwateri versus *P. nasutus*	8.01	8.02
P. attwateri versus *P. gratus*	11.40	10.50
P. attwateri versus *P. truei*	13.30	9.49
P. attwateri versus ingroup	13.10	9.27
P. difficilis versus *P. nasutus*	7.21	5.58
P. difficilis versus *P. gratus*	10.80	9.86
P. difficilis versus *P. truei*	13.20	10.90
P. difficilis versus ingroup	13.00	10.10
P. nasutus versus *P. gratus*	11.50	10.60
P. nasutus versus *P. truei*	12.00	11.10
P. nasutus versus ingroup	12.00	11.10
P. gratus versus *P. truei*	10.40	8.19
Within species		
P. attwateri	-	-
P. difficilis	-	-
P. nasutus	1.00	1.00
P. gratus	2.00	3.00
P. truei	3.00	2.00
P. truei (west)	1.00	-
P. truei (east)	1.00	-
Between subspecies		
P. t. comanche versus *P. t. montipinoris*	4.81	-
P. t. comanche versus *P. t. gilberti*	4.89	-
P. t. comanche versus *P. t. chlorus*	4.99	-
P. t. comanche versus *P. t. martirensis*	4.58	-
P. t. comanche versus *P. t. lagunae*	4.79	-
P. t. comanche versus *P. t. preblei*	4.88	-
P. t. comanche versus *P. t. nevadensis*	3.99	-
P. t. comanche versus *P. t. nevadensis* (west)	4.88	-
P. t. comanche versus *P. t. nevadensis* (east)	1.32	-
P. t. comanche versus *P. t. truei*	3.79	-

Table 1. (cont.)

Peromyscus comparsion	*Cyt*b	D-loop
P. t. comanche versus *P. t. truei* (west)	4.82	-
P. t. comanche versus *P. t. truei* (east)	1.16	-
P. t. truei (west) versus *P. t. truei* (east)	4.79	-
Within subspecies		
P. t. comanche	1.00	1.00
P. t. truei	3.00	-
P. t. truei (west)	1.00	-
P. t. truei (east)	1.00	-
Between populations		
P. t. comanche versus *P. t. truei* (Glenrio, TX)	1.73	-
P. t. comanche versus *P. t. truei* (Black Mesa, OK)	1.0	1.81
P. t. comanche versus *P. t. truei* (Mills Canyon, NM)	0.79	1.7
P. t. comanche versus *P. t. truei* (GUMO, TX)	2.00	-

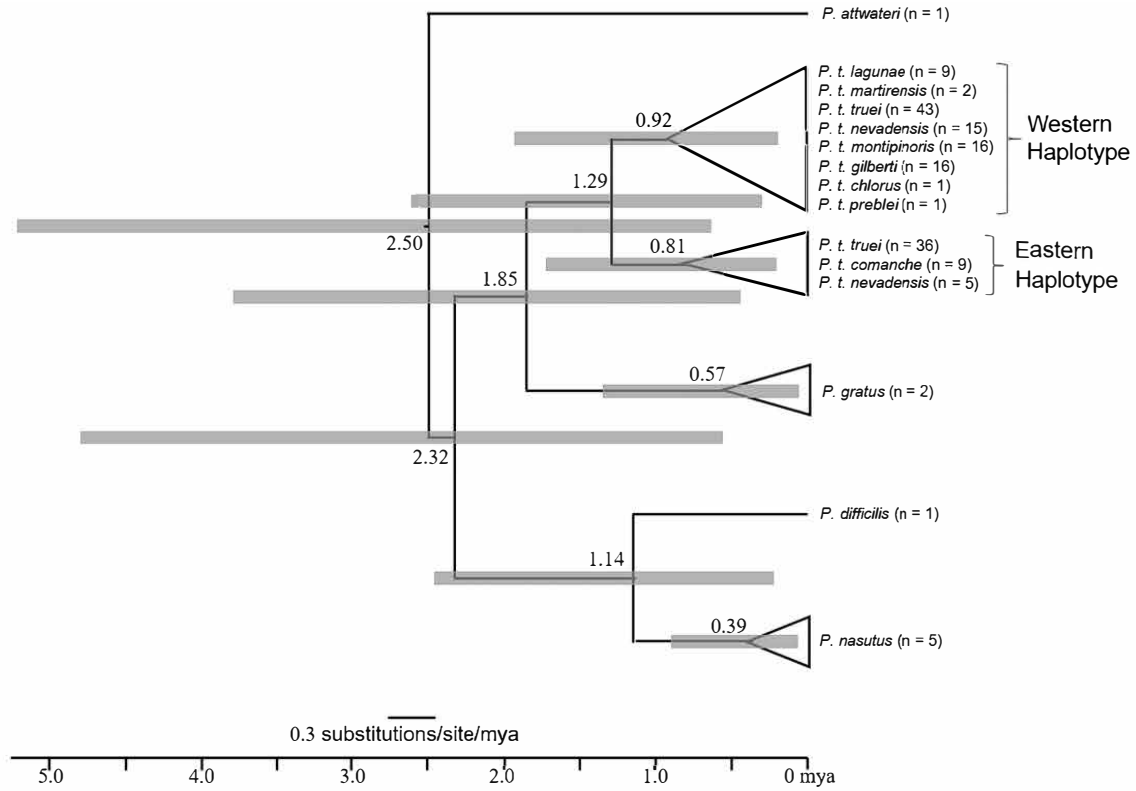

Figure 4. Time-calibrated phylogenetic tree modified from that depicted in Figure 2 with the superimposition of results from the BEAST analysis (Version 2.6.1, Bouckaert et al. 2014) using the mitochondrial cytochrome-*b* gene dataset. Divergence date estimates are indicated along the x-axis in millions of years. Error bars (gray rectangles) represent the 95% highest posterior density for node height.

the majority of the discussion is based on conclusions from the *Cyt*b dataset.

The three populations (Fig. 2; Table 1) associated with the Tule and Palo Duro Canyon region did not form a monophyletic assemblage; nor did they demonstrate geographical affinity to other populations of *P. truei* from northeastern New Mexico, western Oklahoma, or western Texas. However, genetic divergence values suggested a recent evolutionary history of haplotypes associated with *P. t. comanche* to *P. t. truei* haplotypes from Mills Canyon, New Mexico (0.79%) and Black Mesa, Oklahoma (1.00%). This result was unexpected given that the closest *P. truei* population to *P. t. comanche* was the *P. t. truei* samples from Glenrio, Texas (located 120 km to the west) which differed by 1.73%. It is of interest that the Glenrio, Texas, population is by far the closest geographically extant population of *P. t. truei* to those populations of *P. t. comanche* in the Tule and Palo Duro Canyon systems; however, a direct connection of Glenrio, Texas, to the Tule and Palo Duro Canyon systems would require dispersal across an intervening region of the High Plains that has been deemed inhospitable habitat for *P. truei* by Choate (1991, 1997). Further, results from divergence dating analyses suggested that haplotypes associated with samples of *P. t. comanche* from the Texas Panhandle possibly diverged from a source-stock population in northeastern New Mexico approximately 0.71 mya. This infers a possible expansion route (Fig. 5) from Mills Canyon, New Mexico, through canyonlands associated with the Canadian River system along the northeastern edge of the Llano Estacado, and subsequent isolation and divergence of *P. t. comanche* from its *P. t. truei*-like ancestor. At this time, we cannot discern between routes IIA (along the canyonlands of the northeastern edge of the Llano Estacado) or IIB (along the southern major and minor tributaries of the Canadian River system). Although genetic divergence values associated with haplotype similarities between Black Mesa, Oklahoma, and Tule and Palo Duro Canyon were only slightly larger at 1.00% than those obtained from a comparison of haplotypes associated with *P. t. truei* (Mills Canyon, New Mexico, to the Tule and Palo Duro Canyon region) at 0.79%, route III (255 km) from Black Mesa, Oklahoma, to Tule and Palo Duro Canyon is unlikely due to absence of extant populations of *P. truei* along suitable habitat. Similarly, a relatively high level of genetic divergence (2.00%) between haplotypes associated with *P. t. truei* between Guadalupe Mountains National Park, Texas, and Tule and Palo Duro Canyon region in combination with a large intervening geographical distance between localities (445 km) makes route IV unlikely.

Divergence dating analyses indicated that all five focal localities diverged within the last 0.71 mya; therefore, it is reasonable to assume they were part of a continuous population across New Mexico, western Oklahoma, and western Texas. There is historical evidence for a mesic juniper-oak-pinyon pine woodland extending from the Rocky Mountains to the Texas/Mexico border. However, in recent times (0.011 to 0.008 mya), the lower elevation habitats transitioned to a more xeric juniper-dominated landscape, as shown by evidence from packrat middens and pollen (Hafsten 1961; Wells 1966; Johnson and Packard 1974; Wells 1977; Riskind and Van Devender 1979; Van Devender 1990; Stangl et al. 1994; Abbott 1996; Bartlema 2001). In examining the extant *P. truei* populations, Glenrio, Texas, Black Mesa, Oklahoma, and Palo Duro Canyon are more typical of the xeric juniper habitat whereas Mills Canyon, New Mexico, and Guadalupe Mountains National Park, Texas, populations are more similar to habitat associated with *P. truei* populations of the western distribution. Data generated herein do not show a modern-day connection (stepping-stone model) to Glenrio, Texas, and Black Mesa, Oklahoma, to the Tule and Palo Duro Canyon regions. Instead, the genetic divergence data suggests the most recent gene flow occurred from the Mills Canyon, New Mexico, population of *P. t. truei* to the Tule and Palo Duro Canyon population representing *P. t. comanche*. Climatic changes producing a more xeric habitat then isolated the Tule and Palo Duro Canyon region population during the last 0.011 mya, resulting in a relictual population that eventually diverged morphologically to the extent that *P. t. comanche* was recognized as being distinct from *P. t. truei*.

It may be necessary to incorporate advanced genomic techniques to resolve the phylogenetic relationships among the nine subspecies of *P. truei* and to describe the evolutionary history of *P. t. comanche*. Further, sampling from additional localities in eastern New Mexico may provide more information on the presence of the isolated meta-populations of *P. t. comanche*. Although there is no substantial genetic

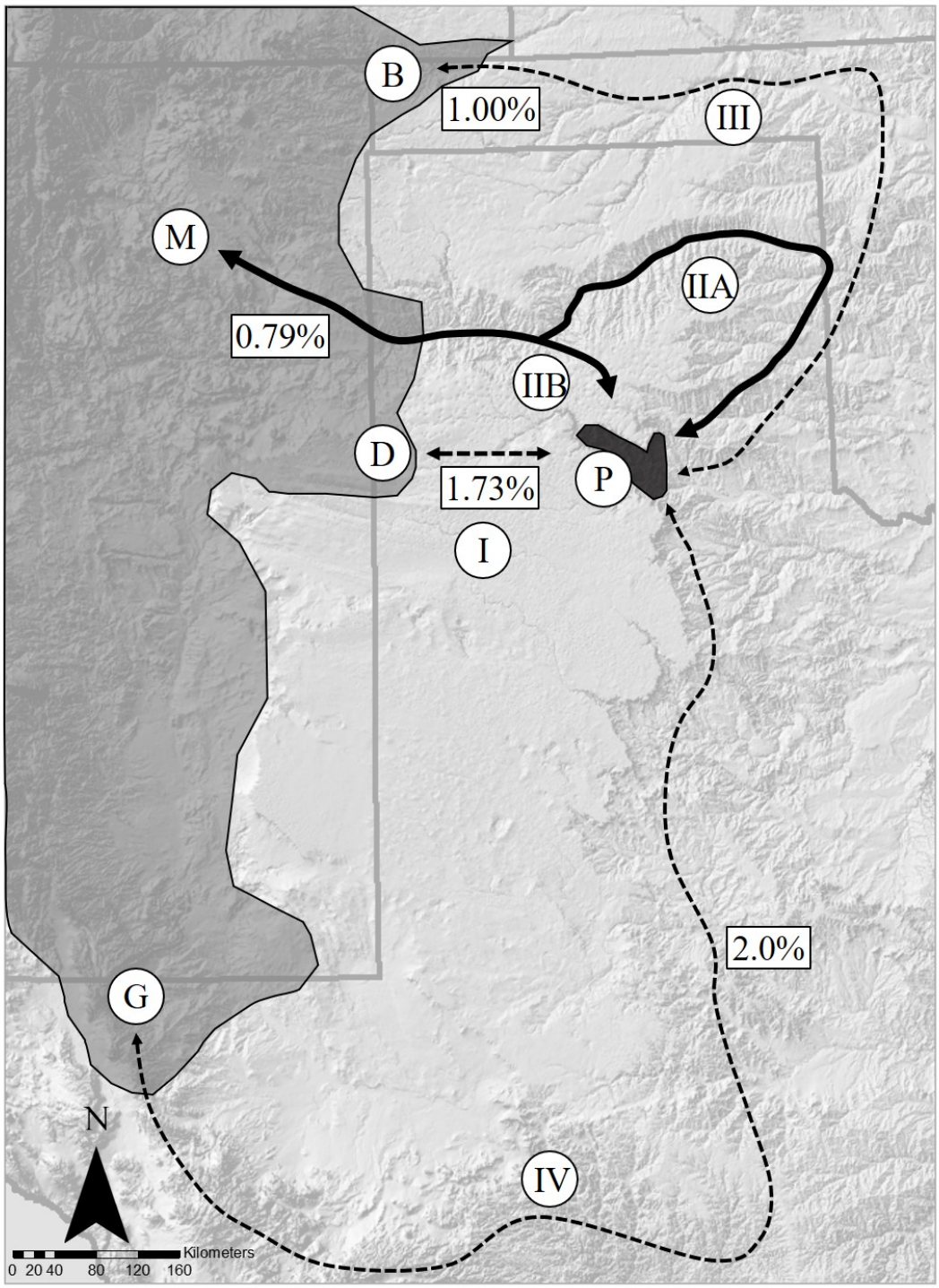

Figure 5. Map depicting the four possible routes from putative source-stock populations of *P. t. truei*. The solid line indicates the most likely pathway (Route IIA or IIB) supported by the Kimura (1980) average genetic divergence values depicted in boxes. Dashed lines represent the three alternate routes (I, III, and IV) discussed in the text. Medium gray shading represents the presumed distribution of *P. t. truei*. Dark gray shading represents the distribution of the *P. t. comanche* population. Localities examined are abbreviated as follows: B = Black Mesa, Oklahoma; M = Mills Canyon, New Mexico; D = Glenrio, Texas; G = Guadalupe Mountains National Park, Texas; and P = Tule and Palo Duro Canyon, Texas.

differentiation between *P. t. comanche* and members of the eastern clade of *P. t. truei* (1.16%), and considering the isolated nature and morphological divergence as depicted by Blair (1943), Hoffmeister (1951), and Schmidly (1973), it seems prudent to continue to recognize *P. t. comanche* as a subspecies until additional data are available.

ACKNOWLEDGMENTS

Thanks to H. J. Garner and K. MacDonald of the Natural Science Research Laboratory, Museum of Texas Tech University, for assisting with tissue loans. Thanks to M. J. Buchholz for assistance with ArcMap. Special thank you to D. S. Rogers and N. Lewis-Rogers for providing easy access to the *Peromyscus truei* sequences deposited in GenBank. Thanks to the Field Methods class of 2014 and 2016 for help with specimen collection. Support for collecting some of these samples was provided by a grant from the National Institutes of Health (DHHS A141435-01 to the late C. F. Fulhorst and R. D. Bradley).

LITERATURE CITATIONS

Abbott, J. T. 1996. Natural environment. In: Significance standards for prehistoric archeological sites at Fort Bliss: A design for further research and the management of cultural resources, pp. 9–43. TRC Mariah Associates Inc., Austin, Texas.

Baker, R. J., and R. D. Bradley. 2006. Speciation in mammals and the genetic species concept. Journal of Mammalogy 87:643–662.

Bartlema, L. L. 2001. The Holocene fauna of Big Manhole Cave and its paleoclimatic implications. Master's thesis, University of Texas at El Paso.

Bickham, J. W., C. C. Wood, and J. C. Patton. 1995. Biogeographic implications of cytochrome *b* sequences and allozymes in sockeye (*Oncorhynchus nerka*). Journal of Heredity 86:140–144.

Bickham, J. W., J. C. Patton, D. A. Schlitterm, I. L. Rautenbach, and R. L. Honeycutt. 2004. Molecular phylogenetics, karyotypic diversity, and partition of the genus *Myotis* (Chiroptera: Vespertilionidae). Molecular Phylogenetics and Evolution 33:333–338.

Blair, W. 1943. Biological and morphological distinctness of a previously undescribed species of the *Peromyscus truei* group from Texas. Contributions from the Laboratory of Vertebrate Biology, University of Michigan 24:1–8.

Bouckaert, R., J. Heled, D. Kühnert T. Vaughan,C. H. Wu, D. Xie, A. B. Suchard, and A. J. Drummond. 2014. BEAST 2: a software platform for Bayesian evolutionary analysis. PLoS Computational Biology 10:1–6.

Bradley, R. D., and R. J. Baker. 2001. A test of the genetic species concept: cytochrome-*b* sequences and mammals. Journal of Mammalogy 82:960–973.

Bradley, R. D., D. S. Carroll, M. H. Haynie, R. M. Martinez, M. J. Hamilton, and C. W. Kilpatrick. 2004. A new species of *Peromyscus* from western Mexico. Journal of Mammalogy 85:1184–1193.

Bradley, R. D., J. Q. Francis, R. N. Platt II, T. J. Soniat, D. Alvarez, and L. L. Lindsey. 2019. Mitochondrial DNA sequence data indicate evidence for multiple species within *Peromyscus maniculatus*. Special Publications, Museum of Texas Tech University 70:1–59.

Caire, W., J. D. Tyler, B.P. Glass, and M. A. Mares. 1989. Mammals of Oklahoma. University of Oklahoma Press, Norman.

Castro-Campillo, A., H. R. Roberts, D. J. Schmidly, and R. D. Bradley. 1999. Systematic status of *Peromyscus boylii ambiguous* based on morphologic and molecular data. Journal of Mammalogy 80:1214–1231.

Choate, L. L. 1991. Distribution and natural history of mammals on the Llano Estacado of western Texas and eastern New Mexico. Dissertations, Texas Tech University, Lubbock.

Choate, L. L. 1997. The mammals of the Llano Estacado. Special Publications, Museum of Texas Tech University 40:1–240.

Choate, L. L., R. W. Manning, J. K. Jones, Jr., C. Jones, and T. R. Mollhagen. 1991. Records of mammals for the Llano Estacado and adjacent areas of Texas and New Mexico. Occasional Papers, Museum of Texas Tech University 138:1–11.

Curry, C. J., and J. N. Derr. 2019. Development of lion miniSTRs for use with modern and historical DNA samples. African Journal of Wildlife Research 49:64–74.

Dalquest, W. W. 1962. The Good Creek formation, Pleistocene of Texas, and its fauna. Journal of Paleontology 36:568–582.

Darriba, D., G. L. Taboada, R. Doallo, and D. Posada. 2012. jModelTest 2: more models, new heuristics and parallel computing. Nature Methods 9:772.

DeWalt, T. S., E. G. Zimmerman, and J. V. Planz. 1993. Mitochondrial-DNA phylogeny of species of the *boylii* and *truei* groups of the genus *Peromyscus*. Journal of Mammalogy 74:352–362.

Durish, N. D., K. E. Halcomb, C. W. Kilpatrick, and R. D. Bradley. 2004. Molecular systematics of the *Peromyscus truei* species group. Journal of Mammalogy 85:1160–1169.

Edwards, C.W., C. F. Fulhorst, and R. D. Bradley. 2001. Molecular phylogenetics of the *Neotoma albigula* species group: further evidence of a paraphyletic assemblage. Journal of Mammalogy 82: 267–279.

Findley, J. S., A. H. Harris, D. E. Wilson, and C. Jones. 1975. Mammals of New Mexico. University of New Mexico Press, Albuquerque.

Gould, C. N. 1907. The geology and water resources of the western portion of the Panhandle of Texas. Water Supply and Irrigation 191:1–70.

Hafner, M. S., W. L. Gannon, J. Salazar-Bravo, and S. T. Álvarez-Castañeda. 1997. Mammal collections in the western hemisphere: a survey and directory of existing collections. Allen Press, Lawrence, Kansas.

Hafsten, U. 1961. Pleistocene development of vegetation and climate in the southern High Plains as evidenced by pollen analysis. Pp. 59–91 in Paleoecology of the Llano Estacado. Museum of New Mexico, Santa Fe., Ft. Burgwin Research Center Publication 1.

Hall, E. R. 1981. The mammals of North America. 2nd edition. John Wiley & Sons, New York.

Hoffmeister, D. F. 1951. A taxonomic and evolutionary study of the piñon mouse, *Peromyscus truei*. Illinois Biological Monographs 21:1–104.

Hoffmeister, D. F. 1981. *Peromyscus truei*. American Society of Mammalogists, Mammalian Species 161:1–5.

Hoffmeister, D. F., and L. de la Torre. 1961. Geographic variation in the mouse *Peromyscus difficilis*. Journal of Mammalogy 42:1–13.

Johnson, G. L., and R. L. Packard. 1974. Electrophoretic analysis of *Peromyscus comanche* Blair, with comments on its systematic status. Occasional Papers, Museum of Texas Tech University 24:1–16.

Karow, P. F., G. S. Morgan, R. W. Portell, E. Simmons, and K. Auffenberg. 1996. Middle Pleistocene (early Rancholabrean) vertebrates and associated marine and non-marine invertebrates from Oldsmar, Pinellas County, Florida. Pp. 97–133 in Palaeoecology and palaeoenvironments of Late Cenozoic mammals: Tributes to the career of C. S. (Rufus) Churcher (K. Stewart and K. Seymour, eds.). University of Toronto Press, Toronto, Canada.

Kimura, M. 1953. 'Stepping stone' model of population structure. Annual Report of the National Institute of Genetics, Japan 3:62–63.

Kimura, M., and G. H. Weiss. 1964. The stepping stone model of population structure and the decrease of genetic correlation with distance. Genetics 49:561–576.

Kimura, M. 1980. A simple method for estimating evolutionary rates of base substitutions through comparative studies of nucleotide sequences. Journal of Molecular Evolution 16:111–120.

Kumar, S., G. Stecher, M. Li, C. Knyaz, and K. Tamura. 2018. MEGA X: Molecular Evolutionary Genetics Analysis across computing platforms. Molecular Biology and Evolution 35:1547–1549.

Méndez-Harclerode, F. M., J. D. Hanson, C. F. Fulhorst, M. L. Milazzo, D. C. Ruthven, and R. D. Bradley. 2005. Genetic diversity within the southern plains woodrat (*Neotoma micropus*) in Southern Texas. Journal of Mammalogy 86:180–190.

Modi, W. S., and M. R. Lee. 1984. Systematic implications of chromosomal banding analyses of populations of *Peromyscus truei* (Rodentia: Muridae). Proceedings of the Biological Society of Washington 97:716–723.

Ordóñez-Garza, N., C. W. Thompson, M. K. Unkefer, C. W. Edwards, J. G. Owen, and R. D. Bradley. 2014. Systematics of the *Neotoma mexicana* species group (Mammalia: Rodentia: Cricetidae) in Mesoamerica: new molecular evidence on the status and relationships of *N. ferruginea* Tomes, 1862. Proceedings of the Biological Society of Washington 127:518–532.

Peppers, L.L., and R. D. Bradley. 2000. Cryptic species in *Sigmodon hispidus*: evidence from DNA sequences. Journal of Mammalogy 81:332–343.

Peppers, L. L., D. S. Carroll, and R. D. Bradley. 2002. Molecular systematics of the genus *Sigmodon* (Rodentia: Muridae): evidence from the mitochondrial cytochrome-*b* gene. Journal of Mammalogy 83:396–407.

Platt II, R. N., B. R. Amman, M. S. Keith, C. W. Thompson, and R. D. Bradley. 2015. What is *Peromyscus*?

Evidence from nuclear and mitochondrial DNA sequences suggest the need for a new classification. Journal of Mammalogy 96:708–719.

Riskind, D. H., and T. R. Van Devender. 1979. Pack rats: Unwitting helpers of archeologists. Texas Parks and Wildlife 37:6–9.

Rodhouse, T. J., R. P. Hirnyck, and R. G. Wright. 2010. Habitat selection of rodents along a piñon-juniper woodland-savannah gradient. Journal of Mammalogy 91:447–457.

Rogers, D. S., N. Lewis-Rogers, S. Lewis-Rogers, S. T. Álvarez-Castañeda, and E. A. Rickart. 2019. Mitochondrial cytochrome-*b* variation within *Peromyscus truei* reveals two strongly divergent haplogroups. Pp. 577–612 in From field to laboratory: a memorial volume in honor of Robert J. Baker (R. D. Bradley, H. H. Genoways, D. J. Schmidly, and L. C. Bradley, eds.). Special Publications, Museum of Texas Tech University 71:1–911.

Ronquist, F., M. Teslenko, P. van der Mark, D. L. Ayers, A. Darling, S. Hohna, B. Larget, L. Liu, M. A. Suchard, and J. P. Huelsenbeck. 2012. MrBayes 3.2: Efficient Bayesian phylogenetic inference and model choice across a large model space. Systematic Biology 61:539–542.

Saiki, R. K., D. H. Gelfand, S. Stoffel, S. J. Scharf, R. Higuchi, G. T. Horn, K. B. Mullis, and H. A. Erlich. 1988. Primer-directed enzymatic amplification of DNA with a thermostable DNA polymerase. Science 239:487–491.

Schenk, J. J., K. C. Rowe, and S. J. Steppan. 2013. Ecological opportunity and incumbency in the diversification of repeated continental colonizations by Muroid rodents. Systematic Biology 62:837–864.

Schmidly, D. J. 1973. The systematic status of *Peromyscus comanche*. Southwestern Naturalist 18:269–278.

Schmidly, D. J., and R. D. Bradley. 2016. The mammals of Texas. University of Texas Press, Austin.

Smith, M. F., and J. L. Patton. 1999. Phylogenetic relationships and the radiation of Sigmodontine rodents in South America: evidence from Cytochrome-*b*. Journal of Mammalian Evolution 6:89–128.

Sikes, R. S., and Animal Care and Use Committee of the American Society of Mammalogists. 2016. 2016 guidelines of the American Society of Mammalogists for the use of wild mammals in research and education. Journal of Mammalogy 97:663–688.

Stangl, F. B., W. W. Dalquest, and R. R. Hollander. 1994. Evolution of a desert mammalian fauna: A 10,000-year history of mammals from Culberson and Jeff Davis counties, Trans-Pecos Texas. Midwestern State University Press, Wichita Falls, Texas.

Sullivan, K. A. M., R. N. Platt II, R. D. Bradley, and D. A. Ray. 2017. Whole mitochondrial genomes provide increased resolution and indicate paraphyly in deer mice. BMC Zoology 2:11–17.

Swofford, D. L. 2003. PAUP*. Phylogenetic Analysis Using Parsimony (*and Other Methods). Version 4. Sinauer Associates, Sunderland, Massachusetts.

Tiemann-Boege, I. C., C. W. Kilpatrick, D. J. Schmidly, and R. D. Bradley. 2000. Molecular phylogenetics of the *Peromyscus boylii* species group (Rodentia: Muridae) based on mitochondrial cytochrome-*b* sequences. Molecular Phylogenetics and Evolution 16:366–378.

Van Devender, T. R. 1990. Late Quaternary vegetation and climate of the Chihuahuan Desert, United States and Mexico. Pp. 104-133 in Packrat middens: The last 40,000 years of biotic change (J. L. Betancourt, T. R. Van Devender, and P. S. Martin, eds). University of Arizona Press, Tucson.

Wells, P. V. 1966. Late Pleistocene vegetation and degree of pluvial climatic change in the Chihuahuan Desert. Science 153:970–975.

Wells, P. V. 1977. Post-glacial origin of the present Chihuahuan Desert less than 11,500 years ago. Pp. 67–81 in Transactions of the symposium on the biological resources of the Chihuahuan Desert Region, United States, and Mexico (R. H. Wauer and D. H. Riskind, eds.). National Park Service Transactions and Proceedings Series 3, Chihuahuan Desert Research Institute, Alpine, Texas.

Whiting, A. S., A. M. Bauer, and J. W. Sites, Jr. 2003. Phylogenetic relationships and limb loss in sub-Saharan African scincine lizards (Squamata: Scincidae). Molecular Phylogenetics and Evolution 29:582–598.

Yang, D., Y. Song, J. Ma, P. Li, H. Zhang, M. Stanley-Price, C. Li, and Z. Jiang. 2016. Stepping-stones and dispersal flow: establishment of a meta-population of Milu (*Elaphurus davidianus*) through natural re-wilding. Scientific Reports 6:27297.

Addresses of authors:

EMILY A. WRIGHT

Department of Biological Sciences
Texas Tech University
Lubbock, TX 79409-3131
emily.a.wright@ttu.edu

EMMA K. ROBERTS

Department of Biological Sciences
Texas Tech University
Lubbock, TX 79409-3131
emma.k.roberts@ttu.edu

COURTNEY A. EVANS

Department of Biological Sciences
Texas Tech University
Lubbock, TX 79409-3131
courtneyevans01@gmail.com

DAVID J. SCHMIDLY

Retired Emeritus Professor
Texas Tech University
University of New Mexico
60 Homesteads Road
Placitas, NM 87043
djschmidly@gmail.com

ROBERT D. BRADLEY

Department of Biological Sciences and the Museum
Texas Tech University
Lubbock, TX 79409-3131
robert.bradley@ttu.edu

APPENDIX

Specimens examined.—Specimens examined in this study are listed below. For each specimen, the general collecting locality is provided; all specimens were collected from the United States unless otherwise noted. For most taxa, the museum catalog number (abbreviations for museum acronyms follow Hafner et al. 1997) and GenBank accession numbers for *Cyt*b, and D-loop are provided in parentheses and are separated by slashes, respectively. Multiple specimens from the same locality are separated by a semicolon. However, for samples of *P. truei comanche* and *P. t. truei*, the assigned locality, catalog number, and GenBank accession numbers for *Cyt*b and D-loop are listed in parentheses and separated by slashes, respectively. Abbreviations are as follows: Carnegie Museum of Natural History (CM); Museum of Texas Tech University (TTU); Museum of Vertebrate Zoology at Berkeley (MVZ); Centro de Investigaciones Biológicas del Noroeste (CIB); University of Utah, Natural History Museum of Utah (UMNH); Brigham Young University, Monte L. Bean Life Science Museum (BYU); and University of Washington, Thomas Burke Memorial Washington State Museum (UWMB). The following specimens were sequenced for both *Cyt*b and D-loop unless otherwise noted (NA).

Peromyscus attwateri.—Oklahoma; McIntosh Co., 3.1 mi E Dustin (TTU55688/AF155384/N/A); Texas; Garza Co., 10 mi S Post (TTU36088/NA/AF081492).

Peromyscus difficilis amplus.—MEXICO: Tlaxcala; 18 km N, 9 km E Apizaco (CM57108/AY387488/MN164782).

Peromyscus gratus gentilis.—MEXICO: Durango; 3.8 mi W Coyotes, Hacienda Coyotes (TTU81621/AY322507/MN164788).

Peromyscus gratus.—New Mexico; Catron Co., Reserve, Gila National Forest (TTU138339/MN022892/MN164789).

Peromyscus nasutus.—New Mexico; Sandoval Co., 4 mi S, 3 mi W Bernalillo (TTU36097/MN022893/MN164784).

Peromyscus nasutus.—Oklahoma; Cimarron Co., Black Mesa Nature Preserve, (TTU136503/MN022894/MN164785; TTU138362/MN022895/MN164786).

Peromyscus nasutus griseus.—New Mexico; Lincoln Co., 4 mi S Carrizozo (TTU78401/AF155399/MN164783).

Peromyscus nasutus nasutus.—Texas; Jeff Davis Co., Mt. Livermore Preserve (TTU78316/AY376426/MN164787).

Peromyscus truei chlorus.—California; San Bernardino Co., Cactus Flat, San Bernardino Mts. (MVZ198708/MK871875/NA).

Peromyscus truei comanche.—Texas, Armstrong Co., 0.75 mi N, 6.25 mi E Wayside (Locality 3; TTU61541/MN022908/MN164806; TTU61543/AY376428/MN164804; TTU61547/AY376429/MN164805); Briscoe Co., 3 mi N Quitaque, Caprock Canyons (Locality 1; TTU47286/MN022915/MN164812; TTU47296/AY376430/MN164808; TTU47300/MN022913/MN164810); 6 mi N, 4 mi W Silverton (Locality 2; TTU36056/MN022912/MN164809; TTU36060/MN022909/MN164815; TTU36064/MN022911/MN164814; TTU36068/MN022910/MN164813); Caprock Canyons State Park (TTU74991/AY376431/MN164807; TTU69561/MN022914/MN164811).

Peromyscus truei gilberti.—California; Alameda Co., Strawberry Canyon (MVZ157329/AF108703/NA); Strawberry Canyon, below Botanical Gardens (MVZ157330/MK871830/NA); Mariposa Co., 5.7 mi SE Coulterville

(MVZ208171/MK871850/NA); Hunter Valley Mountain (MVZ208172/MK871851/NA; MVZ208173/MK871852/NA; MVZ208176/MK871853/NA; MVZ208181/MK871857/NA); Blackstone Creek, 6.5 mi NE Coulterville (MVZ208184/MK871858/NA; MVZ208185/MK871859/NA; MVZ208187/MK871861/NA; MVZ208188/MK871862/NA; MVZ208189/MK871863/NA); Monterey Co., Arroyo Seco, 7 mi SW Greenfield (MVZ195335/MK871867/NA; MVZ195337;MK871868/NA; MVZ195338/MK871869/NA); Shirttail Canyon, 4.8 mi E Soledad (MVZ195341/MK871870/NA).

Peromyscus truei lagunae.—MEXICO: Baja California Sur; Valle de la Laguna, Sierra de la Laguna (CIB10956/MK872276/NA; CIB10959/MK872277/NA); Agua de San Antonio, 9 km N, 26 km E Todos Santos (CIB10962/MK872280/NA; CIB10964/MK872281/NA; CIB10965/MK872282); Los Pinitos, 17.5 km W Santiago (CIB10966/MK872283/NA); Palo Extrano, Sierra de la Laguna (CIB10969/MK872286/NA; CIB10972/MK872288/NA); 4 km N, 22.5 km W Santiago (CIB10982/MK872293/NA).

Peromyscus truei martirensis.—MEXICO: Baja California; Laguna Juarez (CIB3357/MK872273/NA); 10 mi E Rancho Melling (CIB 3367/MK872274/NA).

Peromyscus truei montipinoris.—California; Kern Co., Rancheria Creek, east end Walker Basin (MVZ197314/MK871835/NA; MVZ197315/MK871836/NA; MVZ197316/MK871837/NA; MVZ197317/MK871838/NA); Temblor Range summit on Hwy. 58 (MVZ198606/MK871841/NA; MVZ198607/MK871842/NA; MVZ198608/MK871843/NA; MVZ198610/MK871845/NA); 2 mi NNW Eagle Rest Peak, San Emigido Mts. (MVZ198616/MK871846/NA); Los Angeles Co., Chatsworth Reservoir Park (TTU83290/AY376432/NA); 4.5 mi E (by road) Gorman (MVZ198394/MK871840/NA); 0.4 mi W Gorman (MVZ198392/MK871848/NA; MVZ198393/MK871849/NA); San Luis Obispo Co., 13.3 mi NW (by road) New Cuyama (MVZ196792/MK871877/NA); Ventura Co., mouth Rose Valley (MVZ198613/MK871878/NA; MVZ198612/MK871880/NA).

Peromyscus truei nevadensis.—Idaho; Cassia Co., City of Rocks National Reserve (UWBM79645/FJ800578/NA; UWBM79646/FJ800579/NA; UWBM79674/FJ800582/NA); Nevada; White Pine Co., 5.3 km W Baker (BYU38274/MK871958; BYU38276/MK871960/NA); Utah; Beaver Co., San Francisco Mountains, 1.75 km N, 0.9 km E Frisco Peak summit (UMNH37585/MK871974/NA); Box Elder Co., 3.6 km N, 8.8 km W crystal Peak (BYU40195/MK871983/NA); Carbon Co., 3.3 km E, 2.5 km N Castle Gate (BYU38484/MK871970/NA); Emery Co., 8.8 km S, 0.5 km W Window Blind Peak (BYU40714/MK871826/NA; BYU40706/MK871827/NA; BYU40704/MK872137/NA); 8.05 km N, 12.25 km W Huntington (BYU36684/MK872045/NA; BYU36685/MK872046/NA; BYU36686/MK872047/NA; BYU38038/MK872077/NA); 7.95 km N, 12.30 km W Huntington (BYU36674/MK872065/NA); 12.5 km N, 22.7 km W Last Chance Benches (BYU38489/MK872104/NA); Garfield Co., Grosvenor Arch Day Use Area (BYU20180/MK872032/NA; BYU20181/MK872033/NA); Millard Co., Ferguson Desert Snake Pass Rd., 3.7 km E Shotgun Knoll (BYU24608/MK872107/NA).

Peromyscus truei preblei.—Oregon; Deschutes Co., 5 km W Tumalo (BYU21081/MK871963/NA).

Peromyscus truei truei.—Arizona; Coconino Co., Navajo Nation (BYU41011/MK871823/NA; BYU41012/MK871824/NA; BYU41013/MK871825); Apache Co., (Locality 13; TTU104427/AY376433/MN164793); Navajo Co., 3 mi S Woodruff (Locality 14; TTU78507/AF155412/MN164792); Colorado; Chaffee Co., 7.2 km E, 3.65 km N Poncha Mountain (BYU37099/MK871883/NA); Mesa Co., W Grand Junction, Colorado National Monument (Locality 12; TTU55604/MN022896/MN164790); Fort Carson Co., Camp Red Devil (Locality 7; TTU100425/MN022897/MN164791); Nevada; Clark Co., 1.20 km N, 0.25 km W Willow Spring (BYU39546/MK871887/NA; BYU39550/MK871891/NA; BYU39552/MK871893/NA); 1.10 km N, Willow Spring (BYU39542/MK871896/NA); Willow Creek, 1.24 km N, 0.10 km W Willow Spring (UMNH40544/MK871899/NA; UMNH40545/MK871900/NA); Spring Mountains, Telephone Canyon, 0.4 km S, 4.2 km E summit Fletcher Peak (UMNH40768/MK871910/NA); Mineral Co., Wassuk Range, Cottonwood Creek, 2 mi S, 4 mi W Walker Lake (UMNH39130/

MK871915/NA); Wassuk Range, Cottonwood Creek, 3 km W summit of Mount Grant (UMNH39141/MK871918/NA); Nye Co., Peavine Canyon, 0.92 km N, 0.27 km W mouth Horse Canyon (BYU33806/MK871922/NA); Pine Creek Canyon (BYU34412/MK871925/NA; BYU34413/MK871926/NA; BYU34415/MK871928/NA; BYU34417/MK871930/NA; BYU34418/MK871931/NA; BYU34434/MK871941/NA; BYU34442/MK871949/NA); New Mexico; Catron Co., Quemado, Gila National Forest (Locality 11; TTU119068/MN022899/MN164796; TTU119069/MN022898/MN164795); Socorro Co., 32 mi S, 23.5 mi W Socorro (Locality 10; TTU36053/AY376434/MN164794); Sandoval Co., 4 mi S, 3 mi W Bernalillo (Locality 9; TTU36096/MN022900/MN164797); Harding Co., 9.0 mi SW Mills, Mills Canyon Campground, Kiowa National Grassland (Locality 6; TTU142741/MN022901/MN164798; TTU142742/MN022902/MN164799; TTU142743/MN022903/MN164800); Oklahoma; Cimarron Co., Black Mesa Nature Preserve, (Locality 4; TTU136502/MN022904/MN164801; TTU120630/MN022905/NA; TTU120631/MN022906/MN164802; TTU120632/MN022907/MN164803); Texas; Culberson Co., Upper Dog Ranger Station, Guadalupe Mountains National Park (Locality 8; TTU20584/MT670436/NA); Marcus Cabin, West Dog Canyon, 0.75 mi W, 6.38 mi N Guadalupe Peak, Guadalupe Mountains National Park (Locality X; TTU23544/MT670435/NA); Deaf Smith Co., 10 mi N, 35 mi W Hereford (Locality 5; TTU57016/MT188565/NA); 11 mi S, 2 mi E Glenrio (Locality 5; TTU58045/MT188566/NA); Utah; Garfield Co., Escalante River Trailhead (BYU20114/MK872015/NA); 9.35 km E, 0.20 km N Mount Pennell (BYU35903/MK872115/NA); 5.75 km E, 2.54 km S Steep Creek Bench (BYU35947/MK872186/NA); 11.00 km E, 0.90 km S Steep Creek Bench (BYU35977/MK872188/NA; BYU35978/MK872189/NA;BYU35986/MK872196/NA); 16.30 km E, 5.85 km S Steep Creek Bench (BYU36017/MK872199/NA); Wolverine Petrified Forest (BYU20316/MK872223/NA; BYU20323/MK872224/NA); 0.50 km E, 1.30 km N Wolverine Bench (BYU36047/MK872245/NA; BYU36055/MK872252/NA); Grand Co., 0.25 km S, 0.30 km E Dewey Bridge, south of USA, Colorado River (UMNH38144/MK872000/NA); 0.60 km N, 0.90 km E Dewey Bridge, north of USA, Colorado River (UMNH38127/MK872001/NA); Utah Bottoms, Dolores River (UMNH34767/MK872002/NA; UMNH34775/MK872003/NA; UMNH34776/MK872004/NA; UMNH35706/MK872008/NA; UMNH35708/MK872010/NA); Grand Co., Rio Mesa field station, south side of Dolores River (UMNH38077/MK872006/NA); Kane Co., Buckskin Mountain (BYU23634/MK871969/NA); Camp Flat (BYU23636/MK871977/NA); Dance Hall Rock (BYU20232/MK871989/NA); Devil's Garden (BYU23591/MK871993/NA; BYU23574/MK871995/NA; BYU23577/MK871997/NA); 4.50 km E, 5.30 km S Elephant Butte (BYU37451/MK872012/NA); 6.50 km E, 9.20 km S Flag Point (BYU37475/MK872018/NA; BYU37476/MK872019/NA; BYU37479/MK872022/NA); Fourmile Bench (BYU23644; MK872027/NA); Kitchen Corral (BYU23656/MK872085); No Man's Mesa (BYU23690/MK872122/NA); Smoky Hollow (BYU23731/MK872160/NA); San Juan Co., 0.8 km E, 3.6 km N Navajo Mountain (UMNH43001/MK871828/NA); 4.5 km E, 7.6 km S South Peak, Abajo Mountains (BYU38499/MK871968/NA); La Sal Mtns, tributary to Brumley Creek (UMNH31487/MK872096/NA; UMNH31406/MK872098/NA); Uintah Co., Rat Hole Canyon (BYU17166/MK872130/NA); Wayne Co., Aquarius Plateau, Carcass Creek, 3.0 km S, 0.5 km W Grover (UMNH31082/MK872040/NA); Torrey (UMNH36133/MK872210/NA).

Guest editor for this manuscript was Dr. Richard D. Stevens.

Publications of the Museum of Texas Tech University

Institutional subscriptions to Occasional Papers are available through the Museum of Texas Tech University, attn: NSRL Publications Secretary, Box 43191, Lubbock, TX 79409-3191. Individuals may also purchase separate numbers of the Occasional Papers directly from the Museum of Texas Tech University.

Series Editor: Robert D. Bradley
Production Editor: Lisa Bradley

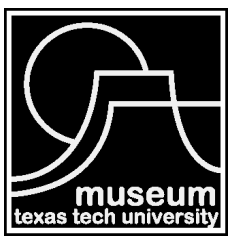

ISSN 0149-175X

Museum of Texas Tech University, Lubbock, TX 79409-3191